EDGEWOOD

CHEMICAL BIOLOGICAL CENTER

U.S. ARMY RESEARCH, DEVELOPMENT AND ENGINEERING COMMAND

ECBC-TR-659

EVALUATION OF MOF-74, MOF-177, and ZIF-8 FOR THE REMOVAL OF TOXIC INDUSTRIAL CHEMICALS

Gregory W. Peterson
John Mahle
Alex Balboa
George Wagner
Tara Sewell
Christopher J. Karwacki

RESEARCH AND TECHNOLOGY DIRECTORATE

November 2008

ABERDEEN PROVING GROUND, MD 21010-5424

Disclaimer

The findings in this report are not to be construed as an official Department of the Army position unless so designated by other authorizing documents.

REPORT DOCUMENTATION PAGE

Form Approved
OMB No. 0704-0188

1. REPORT DATE *(DD-MM-YYYY)*	2. REPORT TYPE	3. DATES COVERED *(From - To)*
XX-11-2008	Final	Feb 2008 - Mar 2008

4. TITLE AND SUBTITLE
Evaluation of MOF-74, MOF-177, and ZIF-8 for the Removal of Toxic Industrial Chemicals

5a. CONTRACT NUMBER

5b. GRANT NUMBER

5c. PROGRAM ELEMENT NUMBER

6. AUTHOR(S)
Peterson, Gregory W.; Mahle, John; Balboa, Alex; Wagner, George; Sewell, Tara; and Karwacki, Christopher J.

5d. PROJECT NUMBER
BA07PRO104

5e. TASK NUMBER

5f. WORK UNIT NUMBER

7. PERFORMING ORGANIZATION NAME(S) AND ADDRESS(ES)
DIR, ECBC, AMSRD-ECB-RT-PF, APG, MD 21010-5424

8. PERFORMING ORGANIZATION REPORT NUMBER
ECBC-TR-659

9. SPONSORING / MONITORING AGENCY NAME(S) AND ADDRESS(ES)
Defense Threat Reduction Agency, 8725 John J. Kingman Road, Room 3226, Fort Belvoir, VA 22060-6201

10. SPONSOR/MONITOR'S ACRONYM(S)
DTRA

11. SPONSOR/MONITOR'S REPORT NUMBER(S)

12. DISTRIBUTION / AVAILABILITY STATEMENT
Approved for public release; distribution is unlimited.

13. SUPPLEMENTARY NOTES

14. ABSTRACT

Current technology-based efforts are focusing on a nanotechnology approach to sorbent development for air purification applications. Metal-organic frameworks (MOFs) and zeolitic imidazolate frameworks (ZIFs) are two novel classes of materials that allow for specific functionalities to be designed directly into a porous framework. This report is the second in a series of summary reports based on the evaluation of samples from the University of California, Los Angeles. The samples evaluated in this report are a continuation of a baseline series of materials aimed at collecting design rules for future materials; results from this and the previous report will be used to create a second-generation of reactive MOFs and ZIFs for air purification applications. Testing of the novel materials included nitrogen isotherm data, water, and chloroethane adsorption equilibria, and ammonia, cyanogen chloride and sulfur dioxide breakthrough data.

15. SUBJECT TERMS

Air purification	Metal-organic frameworks	MOFs	Sorbent development
Nanotechnology	Porous framework	Isotherm	Adsorption equilibria
Breakthrough testing			

16. SECURITY CLASSIFICATION OF:			17. LIMITATION OF ABSTRACT	18. NUMBER OF PAGES	19a. NAME OF RESPONSIBLE PERSON
a. REPORT	b. ABSTRACT	c. THIS PAGE			Sandra J. Johnson
U	U	U	U	38	19b. TELEPHONE NUMBER *(include area code)* (410) 436-2914

Blank

PREFACE

The work described in this report was authorized under Project No. BA07PRO104. This work was started in Feburary 2008 and completed in March 2008.

The use of either trade or manufacturers' names in this report does not constitute an official endorsement of any commercial products. This report may not be cited for the purposes of advertisement.

This report has been approved for public release. Registered users should request additional copies from the Defense Technical Information Center; unregistered users should direct such requests to the National Technical Information Service.

Acknowledgments

The authors thank Omar Yaghi and David Brit (University of California, Los Angeles) for synthesizing the Metal-organic and zeolitic imidazolate framework samples. David Tevault (U.S. Army Edgewood Chemical Biological Center) and Paulette Jones (Science Applications International Corporation) are thanked for their analyses and review of the data and report.

Blank

CONTENTS

FIGURES

TABLES

Blank

EVALUATION OF MOF-74, MOF-177, AND ZIF-8 FOR THE REMOVAL OF TOXIC INDUSTRIAL CHEMICALS

1. INTRODUCTION

In February 2008, Professor Omar Yaghi's group at the University of California, Los Angeles (UCLA), provided two metal-organic framework (MOF) samples and one zeolitic imidazolate framework (ZIF) to the U.S. Army Edgewood Chemical Biological Center (ECBC) for evaluation. Metal-organic frameworks and ZIFs have shown promise for incorporation into air purification technologies due to their ability to modify pore size and functionality on a molecular level. The objective of this evaluation was to assess the physical properties as well as the adsorptive and reactive capabilities of the MOF and ZIF samples in order to provide feedback to Prof. Yaghi's group for the development of new materials. This report provides a summary of the evaluation as well as suggestions for improved MOF/ZIF performance.

The development and evaluation of the MOF and ZIF samples summarized in this report are part of a larger Defense Threat Reduction Agency funded effort to develop novel, nanoscale porous materials for use as sorbents in air purification applications. The objective of this effort is to evaluate the performance characteristics of novel sorbents against a variety of toxic industrial chemicals (TICs) and chemical warfare agents (CWAs) with an emphasis on highly reactive materials that possess broad spectrum filtration capabilities. The goal is to develop materials capable of providing better/broader protection than our current filtration material, ASZM-TEDA, or to complement its filtration properties, possibly leading to composite filters with tailorable performance. If successful, this approach should enable the development of materials and filter designs to purify air via first principles.

This report is the second in a series of summary reports based on the evaluation of samples from UCLA. The first report (Peterson et al., 2008) focused on IRMOF-1 (MOF-5), IRMOF-3, IRMOF-62, and MOF-199 and provided recommendations for future material syntheses. Structures and formulas are provided in Appendix A. The samples evaluated in this report are the continuation of a baseline series of materials aimed at collecting design rules for future materials; results from this report and the previous report will be used to create a second-generation of reactive MOFs and ZIFs for air purification applications.

2. EXPERIMENTAL PROCESS

2.1 Samples Evaluated

The MOF and ZIF samples evaluated are illustrated in Figure 1.

MOF-74

$Zn_3[(O)_3(CO_2)_3]$

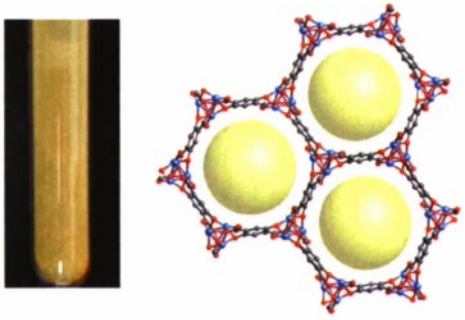

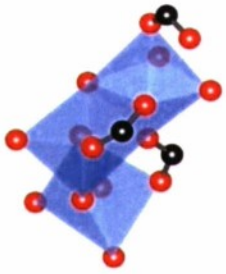

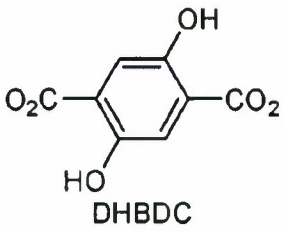

PICTURE *STRUCTURE* *METAL CENTER* (Wong-Foy et al) *LINKER* (Rosi et al)

MOF-177

$Zn_4O(CO_2)_6$

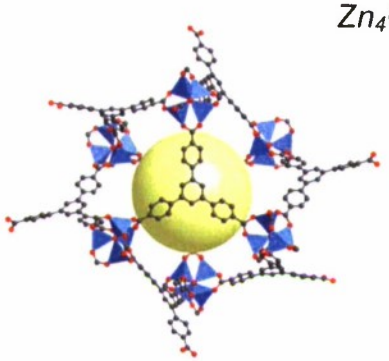

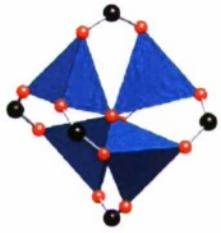

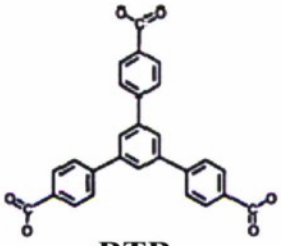

PICTURE *STRUCTURE* (Rowsell et al) *METAL CENTER* *LINKER* (Kim et al.)

ZIF-8: Sodalite Topology

$ZnC_8N_4H_{10}$

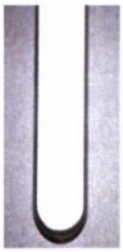

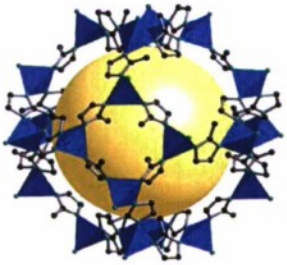

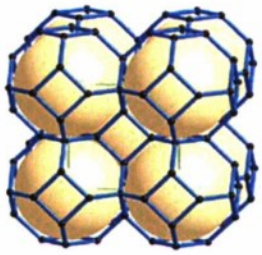

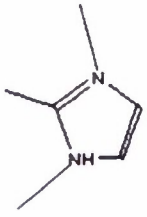

PICTURE *STRUCTURE* (Park et al) *TOPOLOGY* *LINKER*

Figure 1. Samples Evaluated

MOF-74 (ECBC ID# 043-08) is a metal-organic framework that has 3-dimensional rod metal oxides, which form a helical Zn-O-C structure, and 1-dimensional hexagonal channels (Rosi et al., 2005; Rowsell and Yaghi 2006; Liang and Shimizu, 2007). The zinc used in this structure has a coordination number of 6, but is only bonded to 5 oxygen atoms, leaving a highly reactive site. The material received at ECBC was in the form of a yellow-orange powder.

MOF-177 (ECBC ID#044-08) is a metal-organic framework with tetrahedral basic zinc acetate clusters and 1,3,5-benzenetribenzoate (BTB) linkers (Wong-Foy et al., 2006; Li and Yang, 2007) that form a 3-dimensional pore network. The material received at ECBC was in the form of white, flaky, rod-like granules.

ZIF-8 (ECBC ID#024-08) is a zeolitic imidazolate framework that mimics the sodalite topology. The structure consists of Zn^{+2} ions and 2-methylimidazolate in a 1:2 ratio. The empirical formula reported by UCLA is $ZnC_8N_4H_{10}$. The material received at ECBC was in the form of a white powder.

Synthesis procedures for the MOFs studied are summarized in Appendix B (Li et al., 1999; Chae et al., 2004; Rowsell and Yaghi, 2006; Park et al., 2006).

2.2 Testing Protocol

The MOFs were evaluated by collecting the following data: nitrogen isotherm, packing density, temperature and moisture stability, nitrogen and chloroethane adsorption equilibria, and micro-breakthrough testing.

The packing density of each sample was determined in order to summarize data on both a mass and volume basis. Samples were placed in a 10-mm outside diameter glass tube. Dry air was passed through the samples for approximately 4 hr and then weighed. The resulting weight and volume were used to calculate the packing density.

Nitrogen isotherm data were collected with a Quantachrome Autosorb Automated Gas Sorption System. Approximately 20 mg of each MOF were used for the analysis. Samples were outgassed at a temperature of 150 °C for at least 8 hr prior to data measurement. Nitrogen isotherm data were used to estimate the surface area, pore volume, and average pore size.

Chloroethane (CE) adsorption equilibrium (AE) data were collected at 25 °C for the MOF and baseline samples on the system illustrated in Figure 2. The equilibrium system utilizes a Fourier Transform Infrared (FTIR) spectrometer to determine the CE vapor phase concentration, and by inference, CE capacity at different relative pressures. Data are collected based on the vapor concentration difference pre- and post-chemical challenge to a pre-weighed adsorbent and measured volume (i.e., volumetric). Calibrated sample loops provide chemical to the volumetric system in precise quantities. The FTIR spectrometer measures the vapor concentration by partial least squares fit of single and multicomponent chemical vapor concentrations.

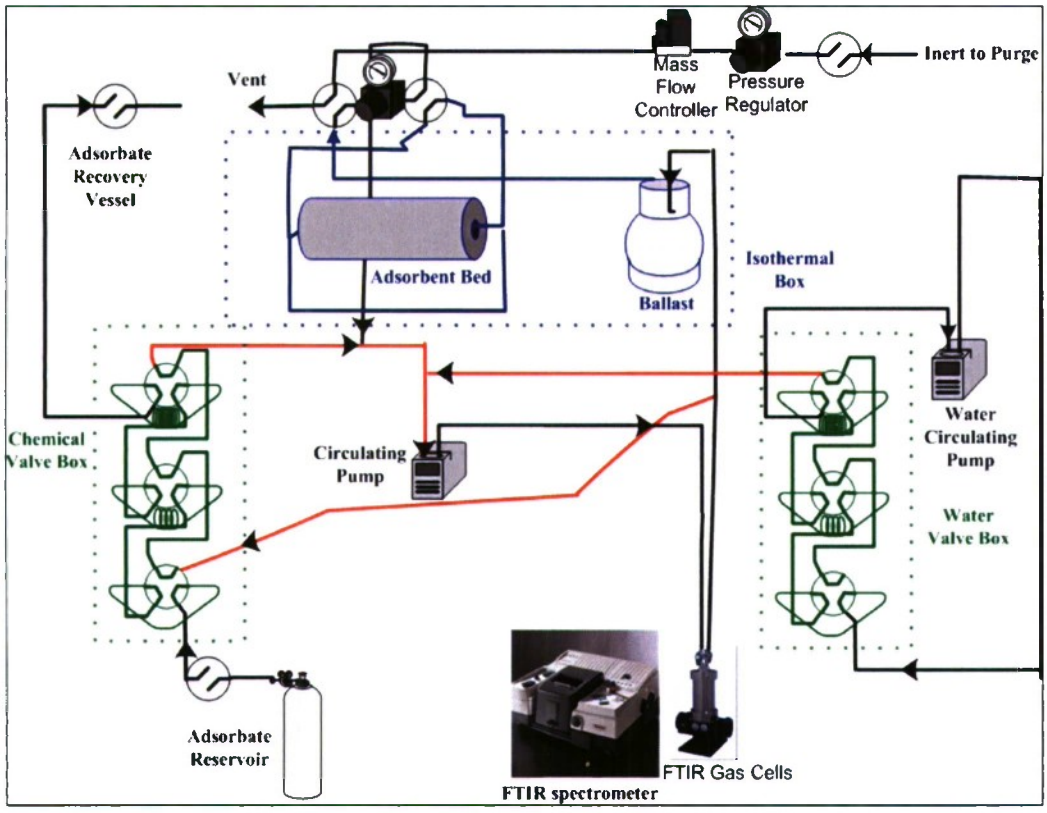

Figure 2. Adsorption Equilibrium System Schematic

Water isotherms were collected on the MOFs and ASZM-TEDA at 25 °C. Water was delivered from a saturator cell to a temperature-controlled microbalance containing the sorbent to be evaluated. The concentration of moisture in the air, or relative humidity (RH), was systematically increased (or decreased) by changing the temperature of the saturator cell. By measuring the change in weight, the amount of water adsorbed on the material was calculated. A system schematic is illustrated in Figure 3.

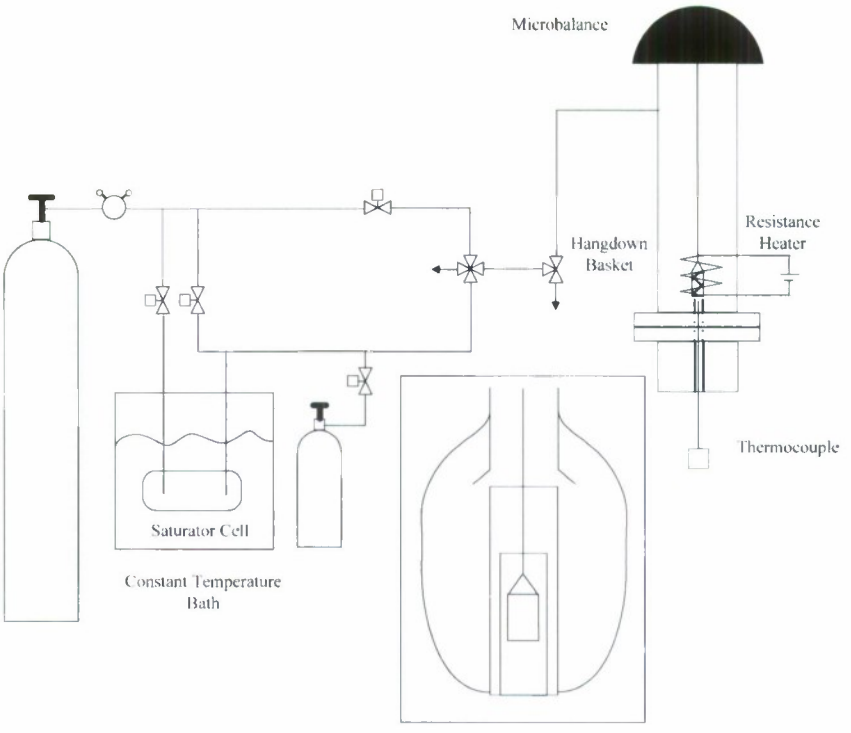

Figure 3. Water Isotherm System

Samples were evaluated for ammonia, cyanogen chloride (CK) and sulfur dioxide capacity using micro-breakthrough systems. A specific amount of chemical was injected into a ballast and subsequently pressurized; this chemical mixture was then mixed with an air stream containing the required moisture content (from a temperature-controlled saturator cell) in order to achieve a predetermined concentration. The completely mixed stream then passed through a sorbent bed submerged in a temperature-controlled water bath. Approximately 20 mg of each sample were tested under dry and humid conditions. The effluent stream then passed through a continuously operating gas chromatograph. A system schematic is shown in Figure 4

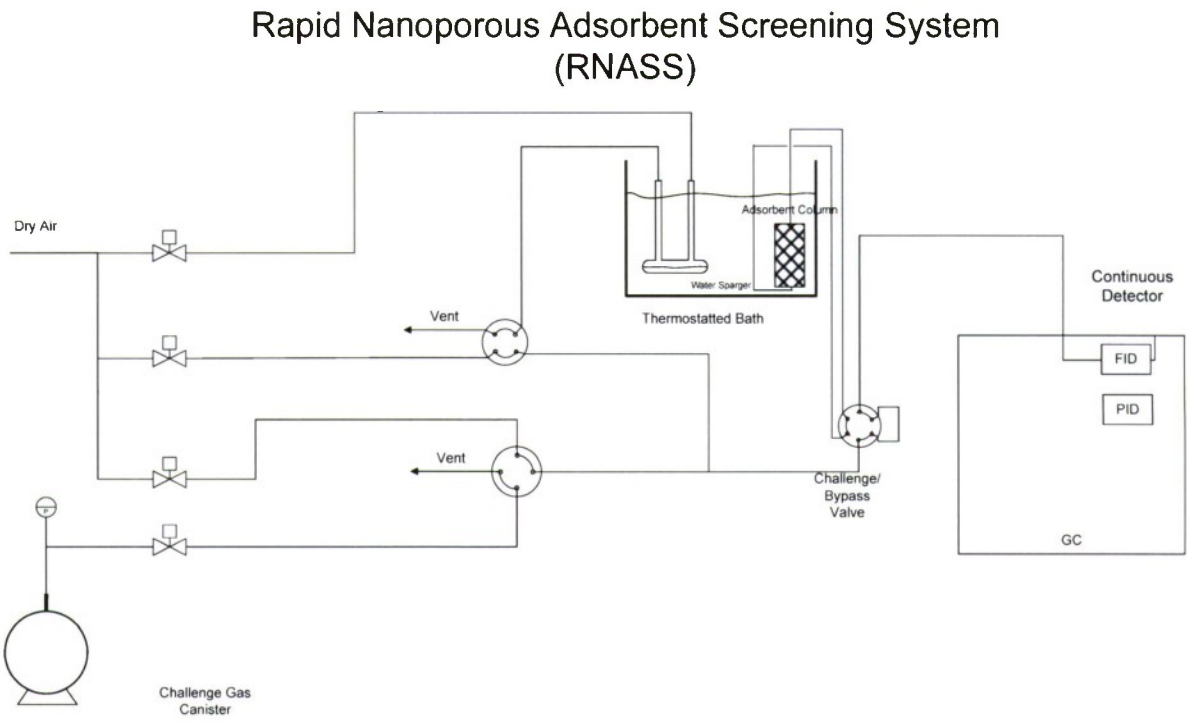

Figure 4. Rapid Nanoporous Adsorbent Screening System

Approximately 50 mm^3 of sorbent were evaluated using an ammonia challenge at a feed concentration of 800 mg/m^3 in air, a bed depth of 4 mm, a flow rate of 20 mL/min (referenced to 25 °C) through a 4 mm tube, and RH of approximately 0% (approximately -40 °C dew point). The residence time (bed volume divided by the flow rate) was approximately 0.15 s. In all cases, sorbents were pre-equilibrated for 1 hr at the same RH as the test. The effluent concentrations were monitored using a photoionization detector (PID).

Approximately 50 mm^3 of sorbent were evaluated using a cyanogen chloride (ClCN or CK) challenge at a feed concentration of 4,000 mg/m^3 in air, a flow rate of 20 mL/min (airflow velocity of approximately 3 cm/s) referenced to 25 °C, a temperature of 20 °C, and relative humidities of approximately 0% and 80%. In all cases, sorbents were pre-equilibrated for approximately 1 hr at the same RH as the test. The effluent concentrations were monitored with a HP5890 Series II Gas Chromatograph equipped with a flame ionization detector (GC/FID).

Approximately 50 mm^3 of sorbent were evaluated with sulfur dioxide at a feed concentration of 1,000 mg/m^3, a flow rate of 20 mL/min (airflow velocity of approximately 3 cm/s) referenced to 25 °C, a temperature of 20 °C, and RHs of approximately 0 and 80%. In all cases, sorbents were pre-equilibrated for 1 hr at the same RH as the test. The concentration eluting through the sorbent was monitored with a HP5890 Series II Gas Chromatograph equipped flame photometric detector (GC/FPD).

3. RESULTS AND DISCUSSION

3.1 Packing Density

The packing density of each sample was calculated in order to summarize data on both a mass and volume basis. Although data are typically reported on a mass basis, filters are designed on a volume basis. The packing density was determined by placing each material in a 10-mm OD glass tube, passing dry air through each sample for approximately 4 hr and then dividing the dry weight by the volume of the material. Packing density measurements are summarized in Table 1.

Table 1. Packing Density of MOFs

Sample	Approximate Mesh	Packing Density
MOF-74	Powder, <70	0.47 g/cc
MOF-177	Powder, <70	0.23 g/cc
ZIF-8	Powder, <70	0.57 g/cc
ASZM-TEDA	12x30	0.61 g/cc

*An actual sieve analysis was not conducted – particle mesh was estimated

All MOF samples received have a significantly lower packing density than ASZM-TEDA. This may become an issue if/when MOFs are used in a filter configuration, as all filters are filled by volume and not mass. Therefore, all properties are reported on both a mass and a volume basis.

3.2 Nitrogen Isotherm

Nitrogen isotherm data were collected with a Quantachrome Autosorb Automated Gas Sorption System. Approximately 50 mg of each MOF was used for the analysis. Samples were outgassed at a temperature of 150 °C for at least 8 hr. Nitrogen isotherm data were collected over six orders of magnitude of relative pressure and then used to estimate the surface area, pore volume and average pore size of MOF samples. Data are illustrated in Figures 5 and 6.

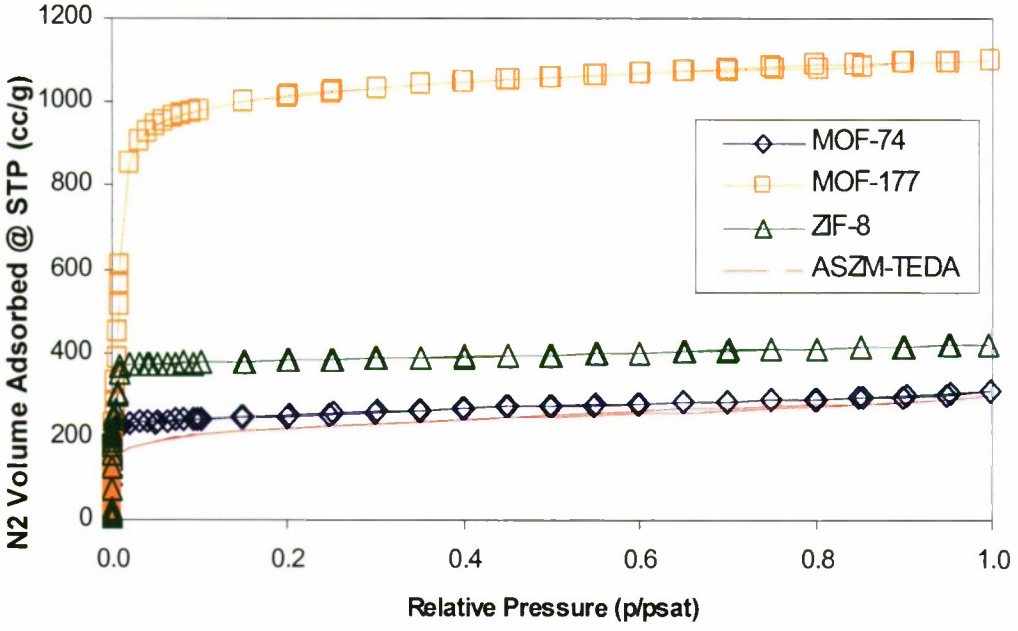

Figure 5. Nitrogen Isotherm Plot

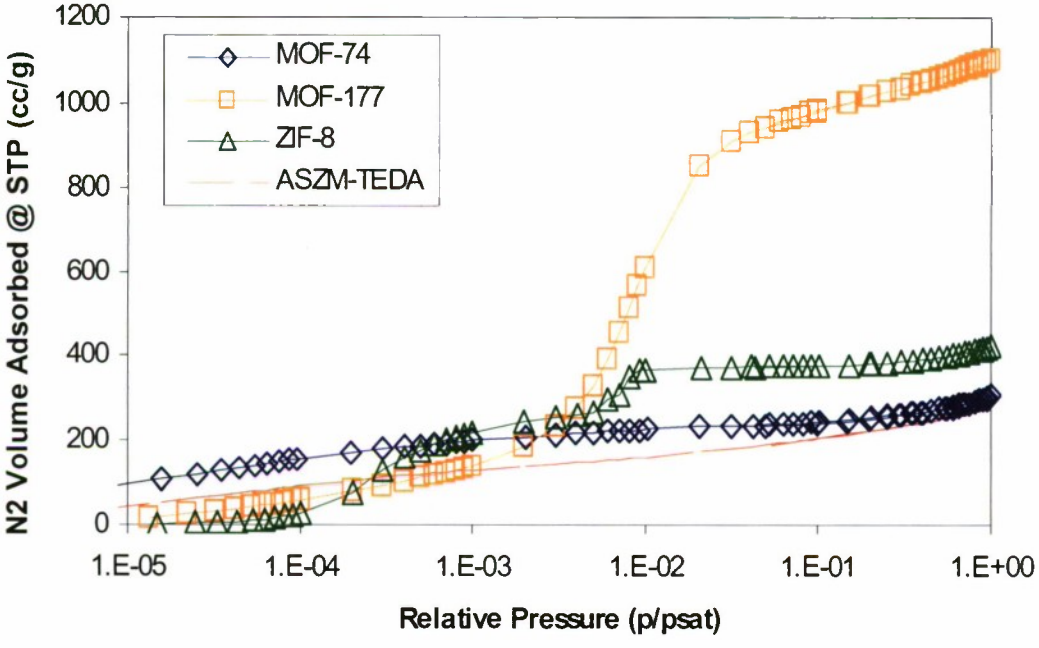

Figure 6. Nitrogen Isotherm Log Plot

All of the samples studied exhibit higher Type I plateaus than ASZM-TEDA, indicating higher BET capacity values and higher nitrogen uptake at higher relative pressures. At low relative pressures, however, only MOF-74 has better nitrogen adsorption properties than ASZM-TEDA, likely due to the higher energy potential created from the open zinc sites. MOF-177 and ZIF-8 have much lower nitrogen adsorption volumes at low relative pressures than either ASZM-TEDA or MOF-74. In MOF-177, this is likely due to the relatively large

distances between metal clusters resulting in low adsorption potentials. However, at higher relative pressures, the very open structure results in very large quantities of nitrogen adsorption compared to the other samples as well as an extremely high BET capacity. In ZIF-8, there is almost no nitrogen adsorption at low relative pressures, possibly due to exclusion from the small pores as well as a lack of adsorption potential. At high relative pressures, however, nitrogen adsorption is much higher than the baseline ASZM-TEDA sample due to the large pore volumes from the supercages.

From the nitrogen isotherm plots, values were calculated for 1/[W((Po/P)-1)] and plotted against relative pressure in order to calculate BET surface area. Fit parameters are summarized in Table 2.

Table 2. Fit Parameters for Calculated BET

Sample	Slope	Y-Intercept	R^2	C
MOF-74	3.517	0.0008189	0.999999	4,295
MOF-177	0.855	0.001442	0.999839	594.1
ZIF-8	2.177	0.001545	0.999034	1,411
ASZM-TEDA	4.224	0.0104300	0.999971	406.1

Nitrogen isotherm data were used to calculate the BET capacity, total pore volume, and average pore size. The term BET capacity, and not surface area, is used for reasons described in the previous Tech Report as well as by Walton and Snurr and Rouquerol et al. The packing density was used to calculate the values on both a mass and volume basis. Table 3 summarizes the calculated values.

Table 3. Calculated BET Capacity and Porosity of MOFs

Sample	BET Capacity		Pore Volume		Pore Width (Å)*	Pore Aperture (Å)*
	m^2/g-adsorbent	m^2/cm^3-adsorbent	cm^3-N_2/g-adsorbent	cm^3-N_2/cm^3-adsorbent		
MOF-74	990	465	0.48	0.23	10.8	10.8
MOF-177	4,065	935	1.73	0.40	11.8	9.6
ZIF-8	1,600	910	0.65	0.37	11.6	3.4
ASZM-TEDA	820	500	0.46	0.28	Heterogeneous**	

*Received from UCLA, calculated based on geometry of unit cell

**Heterogeneous distribution of micropores, mesopores, and macropores

According to the values summarized in Table 3, MOF-74 has similar properties to ASZM-TEDA, with a slightly higher BET capacity and pore volume on a mass basis but a slightly lower BET capacity and pore volume on a volume basis. MOF-177 has an extremely high BET capacity and a wide-open pore network. ZIF-8 has a higher BET capacity and pore volume than ASZM-TEDA; however, the pore width is small and may pose a mass transfer problem in dynamic breakthrough testing.

Professor Yaghi's group also performed BET measurements on the samples sent to ECBC; the results are summarized in Table 4. Tables 5 and 6 summarize the amount of nitrogen adsorbed at various relative pressures.

Table 4. Comparison of ECBC and UCLA Calculated BET Capacity

Sample	ECBC BET Capacity	UCLA BET Capacity	% Difference
MOF-74	990 m^2/g	1,130 m^2/g	+ 14.1%
MOF-177	4,065 m^2/g	4,500 m^2/g	+ 10.7%
ZIF-8	1,600 m^2/g	1,210 m^2/g	- 24.4%

Table 5. Volume of Nitrogen Adsorbed on Selected Materials–Mass Basis

Samples	Volume N_2 Adsorbed (cm^3-STP/g-sorbent)			
	$P/P_0 = 0.001$	$P/P_0 = 0.01$	$P/P_0 = 0.1$	$P/P_0 = 0.3$
MOF-74	200	225	244	260
MOF-177	139	607	981	1,032
ZIF-8	217	367	375	386
ASZM-TEDA	128	161	205	233

Table 6. Volume of Nitrogen Adsorbed on Selected Materials–Volume Basis

Samples	Volume N_2 Adsorbed (cm^3-STP/cm^3-sorbent)			
	$P/P_0 = 0.001$	$P/P_0 = 0.01$	$P/P_0 = 0.1$	$P/P_0 = 0.3$
MOF-74	94	106	115	122
MOF-177	32	140	226	237
ZIF-8	124	209	214	220
ASZM-TEDA	78.1	97.9	125	142

3.3 Chloroethane Adsorption Equilibria (AE)

Chloroethane AE were collected to assess the physical adsorption capacity of MOF samples for light chemicals. Chloroethane was chosen as one of the chemicals of interest due to its similar physical properties with CK, a chemical that is historically filtration-limiting on military air purification sorbents. Chloroethane and CK generally have similar physical adsorption behavior but dissimilar reactive behavior; thus, the potential to differentiate physical and reactive behavior exists. Adsorption Equilibria data for MOF and baseline samples are shown in Figure 7.

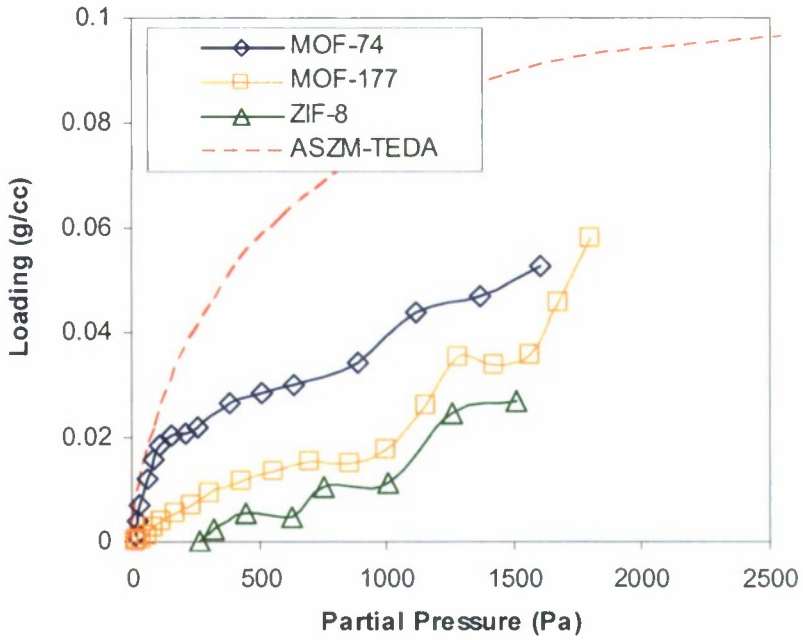

Figure 7. Chloroethane AE at 25 °C Volume Basis

As compared to ASZM-TEDA, the MOF and ZIF samples have a lower chloroethane equilibrium loading over the relative pressure range studied. This was expected for MOF-177 and ZIF-8 as the nitrogen isotherms indicated weak physical adsorption at low relative pressures. The chloroethane capacity for MOF-74 was expected to be higher; however, initially, MOF-74 exhibits similar chloroethane adsorption to ASZM-TEDA, although above approximately 100 Pa, the chloroethane capacity drops off significantly from ASZM-TEDA. This behavior is strange as the surface area and pore volume of MOF-74 is similar to ASZM-TEDA. Perhaps, once a monolayer of chloroethane is formed on MOF-74, the adsorption potential drops significantly due to coverage and interaction with the zinc site.

Chloroethane AE data were used to estimate the equilibrium loadings at three different concentrations (when applicable). Table 7 summarizes the results.

Table 7. Chloroethane Equilibrium Loading (W_E) of Evaluated Samples at 25 °C

Sample	W_E @ 100 mg/m^3 (~38 ppm; $P/P_0 = 2.4 \times 10^{-5}$)		W_E @ 1,000 mg/m^3 (~380 ppm; $P/P_0 = 2.4 \times 10^{-4}$)		W_E @ 10,000 mg/m^3 (~3,800 ppm; $P/P_0 = 2.4 \times 10^{-3}$)	
	g/g	*g/cc*	*g/g*	*g/cc*	*g/g*	*g/cc*
MOF-74	< 0.016	< 0.077	0.016	0.077	0.057	0.027
MOF-177	< 0.0022	< 0.0005	0.0022	0.0005	0.047	0.011
ZIF-8	< 0.0065	< 0.0037	<0.0065	<0.0037	0.0065	0.0037
ASZM-TEDA	0.0039	0.0024	0.020	0.012	0.080	0.049

Of the samples studied, MOF-74 has a significantly higher chloroethane equilibrium capacity at lower relative pressures, and a slightly higher CE capacity than MOF-177 at moderate relative pressures. The unsaturated Zn^{+2} site is likely responsible for this, providing higher adsorption potential. As relative pressures, increase, it is likely that MOF-177 will have higher CE capacities as the pore volume is over three times larger than that of MOF-74. ZIF-8 has a very limited capacity, likely due to the small pore openings.

3.4 Water AE

Water AE were collected on MOF and ZIF samples using a Cahn balance to assess the moisture uptake at a full range of RH conditions. These data will be used to determine if the samples will preferentially adsorb water as opposed to toxic chemicals. AE data for MOF and baseline samples are shown in Figure 8.

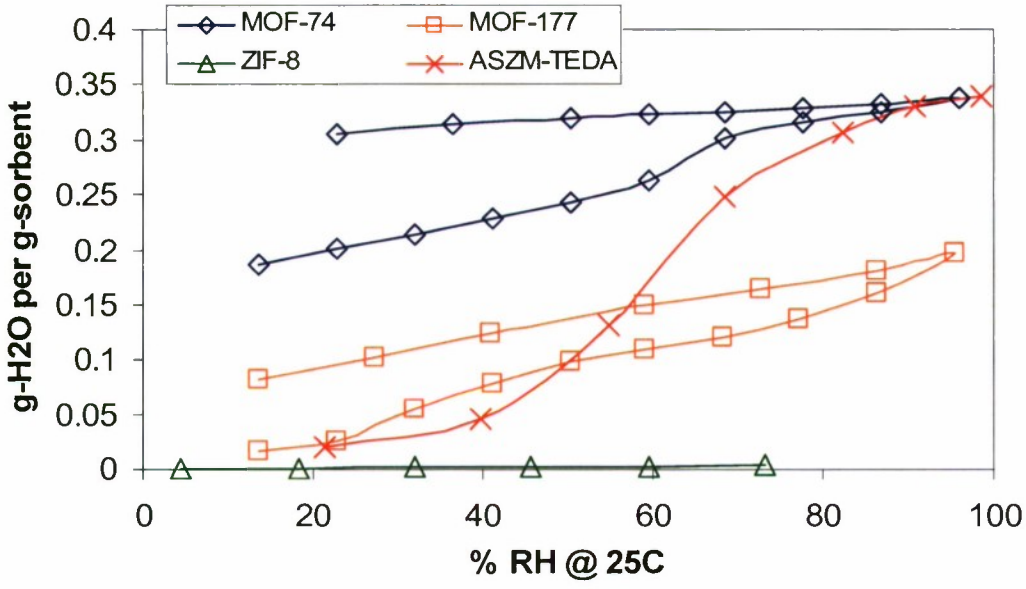

Figure 8. Water AE at 25 °C

As expected, MOF-74 has significant moisture pickup at low RH conditions. This behavior is similar to Cu-BTC (MOF-199), which was evaluated in a previous technical report. The unsaturated metal site (in this case zinc, copper in the case of Cu-BTC) quickly coordinates with any water molecules present in the air stream. MOF-177 shows similar moisture pickup to ASZM-TEDA at low-to-mid RHs; however, ASZM-TEDA picks up significantly more water at high RH conditions. Both MOFs show significant hysteresis, something that we saw with other MOF samples as well. There are two likely explanations for the hysteresis. First, hysteresis may be a measure of pore interconnectivity – the more interconnected the pore network is, the more water acts as a bulk fluid as opposed to a sorbed phase. This translates to a different rate of evaporation (or desorption). The other possible cause of the hysteresis is that it takes a much longer time for a desorbing fluid to reach equilibrium as opposed to an adsorbing fluid; therefore, there may not have been enough elapsed time for the desorption branch to reach equilibrium. Table 8 summarizes the moisture loadings at three RH conditions.

Table 8. Moisture Loading of Sorbents at 25 °C

Sample	Water Loading (g-water/g-sorbent)		
	15% RH	50% RH	80% RH
ASZM-TEDA	0.015	0.088	0.279
MOF-74	0.19	0.24	0.32
MOF-177	0.02	0.10	0.14
ZIF-8	< 0.01	< 0.01	< 0.01

3.5 Ammonia Micro-Breakthrough

Ammonia micro-breakthrough testing was conducted on MOF samples under dry and humid conditions in order to assess ammonia reactive capacity and, more generally, the removal capacity of MOF samples for basic gases. ASZM-TEDA was run as a baseline sample and has a limited ammonia removal capacity. Approximately 50 mm^3 of sorbent were tested at a feed concentration of 800 mg/m^3 in air, a flow rate of 20 mL/min (referenced to 25 °C) through a 4-mm tube, and RH conditions of approximately 0 and 80%. In all cases, sorbents were pre-equilibrated for 1 hr at the same RH as the test. The feed and effluent concentrations were monitored with a PID. Ammonia breakthrough curves under dry RH conditions are illustrated in Figure 9.

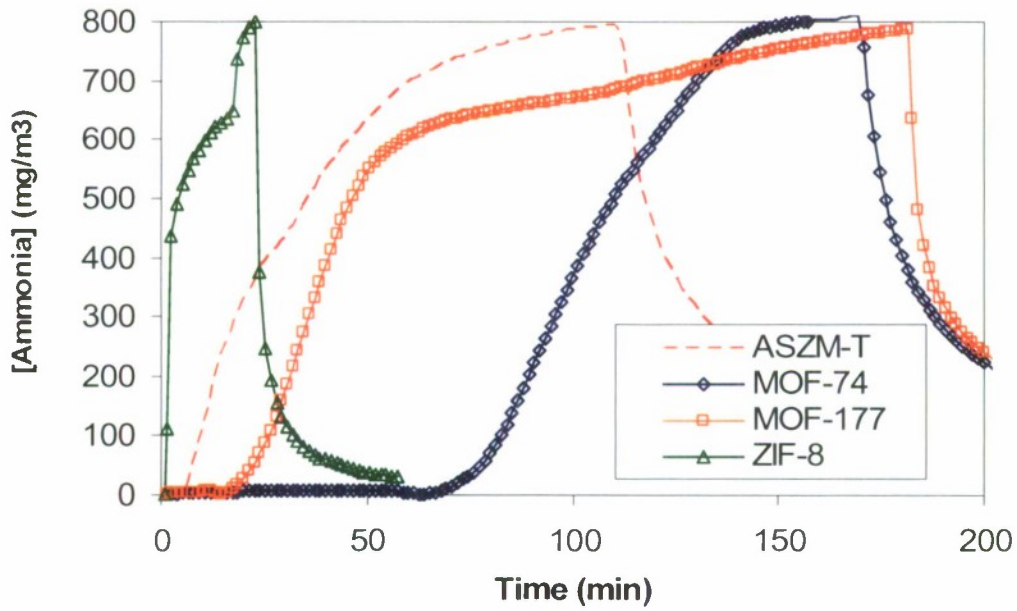

Figure 9. Ammonia Breakthrough Curves under Dry (RH = 0%) Conditions
[Ammonia] ~ 800 mg/m^3

The two MOF samples show some ammonia removal capabilities, which are more extensive than ASZM-TEDA; in MOF-74, the ammonia is likely weakly coordinated to the Zn^{+2} sites, which is supported by the slow initial desorption curve. MOF-177 does not provide an obvious reaction mechanism, but instead likely removes ammonia through initial physical

adsorption followed by ammonia-ammonia interactions; again, this mechanism is supported by the desorption curve. ZIF-8 shows essentially no ammonia removal capabilities, likely due to the combination of very small pore openings and the lack of reactive sites.

Ammonia breakthrough curves under humid (80% RH) conditions are illustrated in Figure 10.

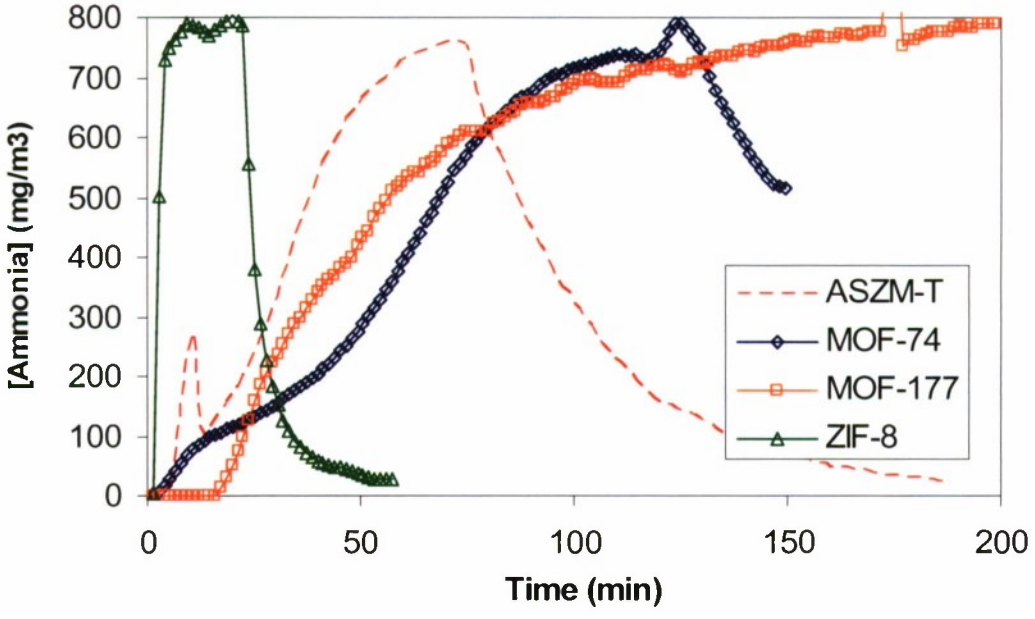

Figure 10. Ammonia Breakthrough Curves under Humid (RH = 80%) Conditions
[Ammonia] ~800 mg/m^3

As under dry conditions, both MOF samples show some ammonia removal capabilities. Although it was expected that the Zn^{+2} sites in MOF-74 would be coordinated and thus shielded by water, it is apparent that ammonia must be preferentially adsorbed; however, there is an initial hump in the breakthrough curve that could be attributed to ammonia-water competition. In MOF-177, it is likely that the extensive water uptake at high RH conditions helps with ammonia removal due to solubility effects, a similar phenomenon to the removal mechanism in ASZM-TEDA. Both MOFs and the ASZM-TEDA show significant desorption, indicating that ammonia removal is not permanent. ZIF-8 shows essentially no ammonia removal capacity, likely due to small pore openings and pre-adsorbed moisture blocking adsorption sites.

Ammonia breakthrough data were used to calculate the dynamic capacity to the stoichiometric center of the breakthrough curve using eqs 1 and 2. The results are summarized in Table 9.

$$Ct = t_B * [Feed] \quad (1)$$

Where Ct = mg-min/m^3
t_B = Breakthrough time [=] min
[Feed] = Feed concentration [=] mg/m^3

$$W_D = \frac{Ct * FR}{Mass} \quad (2)$$

Where W_D = Dynamic capacity [=] g ammonia per g sorbent
FR = Flow rate [=] m^3/min
Mass = Mass of sorbent [=] mg

Table 9. Ammonia Dynamic Capacity of Sorbents

Sample	Sorbent Mass* (mg)	Breakthrough Time to S.C. (min)	W_D to 500 mg/m^3	
			Mass Basis (g/g)	*Volume Basis* (g/cc)*
MOF-74 (Dry)	16.4	103	0.100	0.047
MOF-74 (Wet)	13.5	61	0.073	0.034
MOF-177 (Dry)	19.5	41	0.033	0.008
MOF-177 (Wet)	16.9	48	0.045	0.010
ZIF-8 (Dry)	24.9	2	0.001	0.001
ZIF-8 (Wet)	18.0	3	0.002	0.001
ASZM-TEDA (Dry)	30.0	11	0.025	0.015
ASZM-TEDA (Wet)	25.0	27	0.031	0.019

*Dry basis – does not include mass of loaded water

3.6 CK Micro-Breakthrough

Cyanogen Chloride micro-breakthrough testing was conducted on MOF samples under dry and humid conditions to assess CK reactive capacity. In addition to information on CK removal capabilities, breakthrough curves should indicate the ability of MOFs to remove acid gases. ASZM-TEDA was run as a baseline sample and has a relatively high CK removal capacity. Approximately 50 mm^3 of sorbent were tested at a feed concentration of 4,000 mg/m^3, a flow rate of 20 mL/min (airflow velocity of approximately 3 cm/s) referenced to 25 °C, a temperature of 20 °C, and RHs of approximately 0 and 80%. In all cases, sorbents were pre-equilibrated for approximately 1 hr at the same RH as the test. The feed and effluent concentrations were monitored with an HP5890 Series II GC/FID. CK breakthrough curves for MOF and baseline samples under low-RH conditions are illustrated in Figure 11.

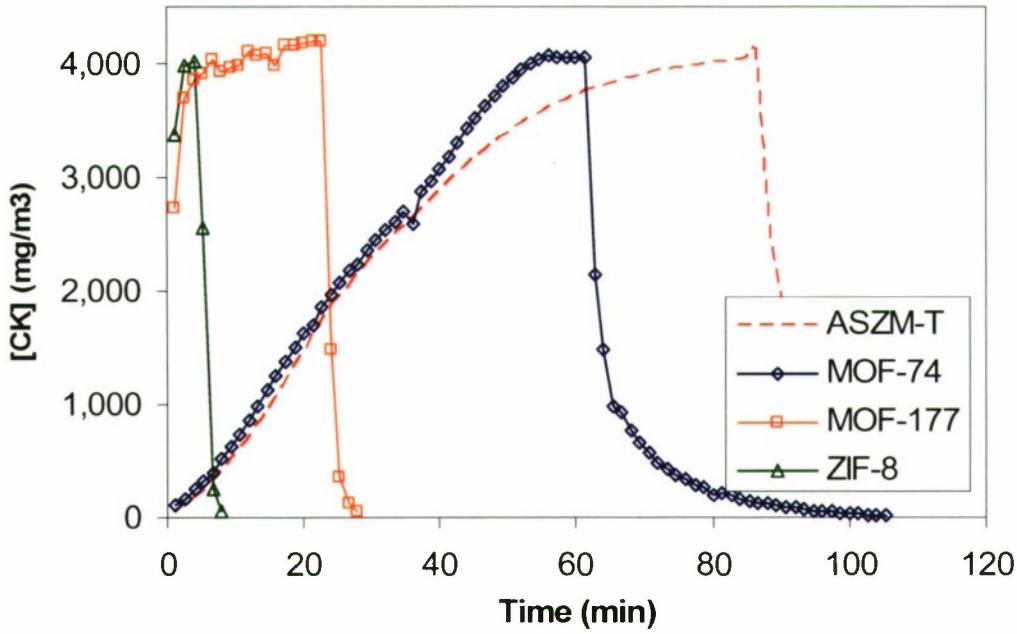

Figure 11. CK Breakthrough Curves under Low RH Conditions
[CK Challenge] = 4,000 mg/m^3

Under low-RH conditions, ASZM-TEDA exhibits some uptake of CK. The shallow ASZM-TEDA breakthrough curve can be attributed to the relatively large particle size (~12-30 US mesh size or 1.7-0.6 mm, respectively) as compared to the MOF samples tested. Under the dry RH conditions, there may be some chemical reaction on ASZM-TEDA; however the primary mechanism for removal is likely physical adsorption, as the effluent concentration does not return to zero immediately following termination of CK challenge. MOF-74 has a similar breakthrough curve to ASZM-TEDA and removal may be due to some chemical reaction with the open Zn^{+2} site. This is supported by the CK effluent concentration quickly returning to the baseline after feed termination. MOF-177 and ZIF-8 show immediate CK breakthrough. In MOF-177, there is no reaction mechanism due to the shielded Zn sites which are spread really thin to promote significant adsorption. In ZIF-8, the combination of small pore openings and lack of reactive sites also results in essentially no CK capacity.

Breakthrough curves for MOF and baseline samples collected under humid (80% RH) conditions are illustrated in Figure 12.

Under humid conditions, ASZM-TEDA, which starts eluting on the far right of the graph, shows extensive CK capacity. This is consistent with previous CK studies as well as the proposed CK reaction mechanism on ASZM-TEDA, which involves hydrolysis. Under humid (80% RH) conditions, all MOF samples exhibit minimal CK removal capacity. Even MOF-74, which exhibits some removal capabilities under dry conditions, does not remove CK at high-RH conditions. The likely degradation mechanism is the hydration of the Zn^{+2} active sites. Because CK is a high vapor pressure chemical (~1,200 torr at 25 °C), it can not compete with preadsorbed moisture for adsorption.

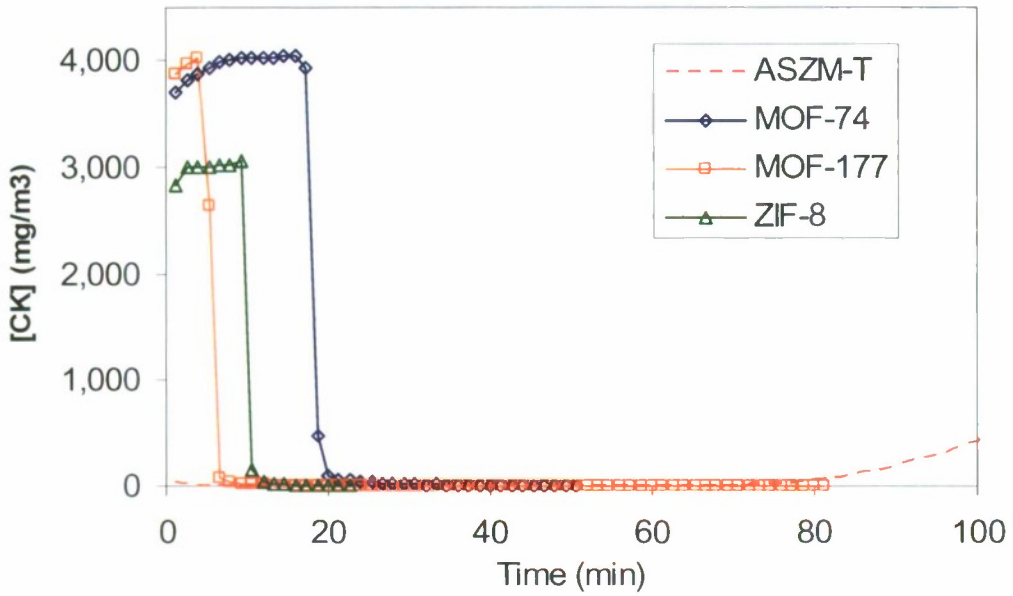

Figure 12. CK Breakthrough Curves under Humid (RH = 80%) Conditions
[CK Challenge] = 4,000 mg/m^3

Breakthrough data on CK were used to calculate the dynamic capacity of the sorbents to the stoichiometric center using the same methodology as was used for ammonia. Results are summarized in Table 10.

Table 10. CK Dynamic Capacity of Sorbents

Sample	Sorbent Mass* (mg)	Breakthrough Time to S.C. (min)	W_D to 2,000 mg/m^3	
			Mass Basis (g/g)	*Volume Basis** (g/cc)
MOF-74 (Dry)	10.1	25	0.197	0.093
MOF-74 (Wet)	13.4	0	0.001	0.001
MOF-177 (Dry)	10.2	1	0.009	0.002
MOF-177 (Wet)	13.3	0	0.001	<0.001
ZIF-8 (Dry)	21.2	0	<0.001	<0.001
ZIF-8 (Wet)	26.6	1	0.002	0.001
ASZM-TEDA (Dry)	15.1	26	0.138	0.084
ASZM-TEDA (Wet)	67.3	143	0.170	0.104

*Dry basis – does not include mass of loaded water

3.7 Sulfur Dioxide Micro-Breakthrough

Sulfur dioxide micro-breakthrough testing was conducted on MOF samples under dry and humid conditions in order to assess sulfur dioxide reactive capacity, and, more generally, the removal capacity of MOF samples for weak acid gases. The assumption is that if MOFs show removal mechanisms for weakly acidic gases, then strong acids should also be removed. ASZM-TEDA was tested as a baseline sample and has a relatively high sulfur dioxide removal capacity. Approximately 50 mm^3 of sorbent were tested at a feed concentration of 1,000 mg/m^3, a flow rate of 20 mL/min (airflow velocity of approximately 3 cm/s) referenced to 760 Torr and 25 °C, a temperature of 20 °C, and RHs of approximately 0 and 80%. In all cases, sorbents were pre-equilibrated for 1 hr at the same RH as the test. The concentration eluting through the sorbent was monitored with an FPD. Sulfur dioxide breakthrough curves for MOF and baseline samples are illustrated in Figures 13 and 14.

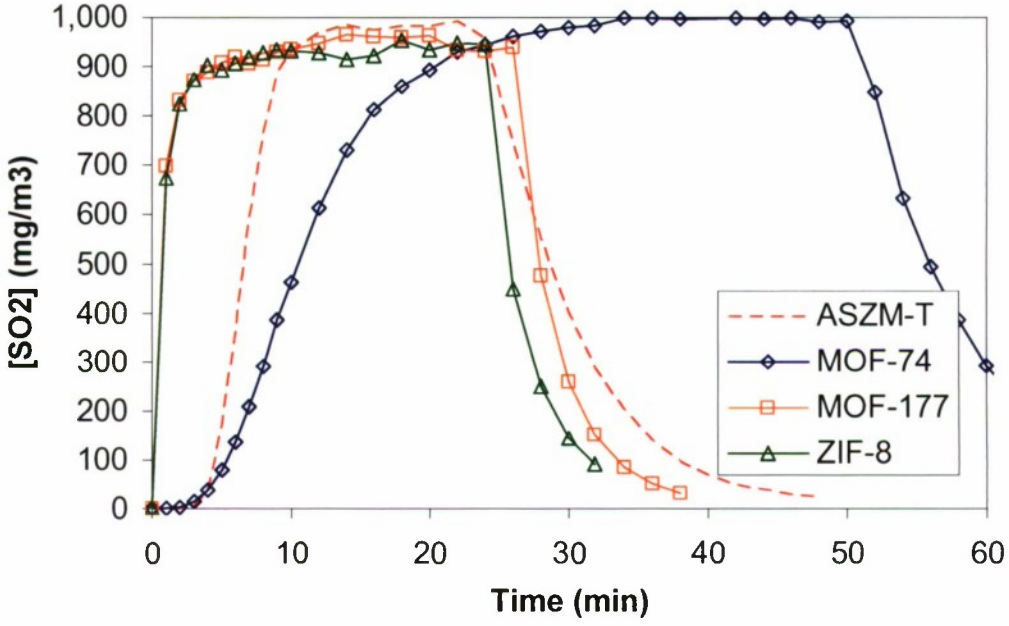

Figure 13. SO_2 Breakthrough Curves under Dry (RH = 0%) Conditions
[Challenge] = 1,000 mg/m^3

Under dry RH conditions, both ASZM-TEDA and MOF-74 exhibit some SO_2 removal; copper and zinc impregnants are responsible for SO_2 removal in ASZM-TEDA while it is likely that the unsaturated zinc site promotes a coordination reaction in MOF-74. In both cases, it is apparent from the desorption curves that both removal mechanisms are reversible, as a substantial amount of SO_2 elutes after feed termination. Neither MOF-177 nor ZIF-8 provides any substantial protection against SO_2 under dry RH conditions and the feed concentration is reached almost immediately for both samples. The covered zinc sites in MOF-177 are unable to provide any reaction mechanism for SO_2, and it is possible that the pores in ZIF-8 are so small that mass transfer into the pores is inhibited.

Figure 14 shows SO_2 breakthrough curves under high RH conditions.

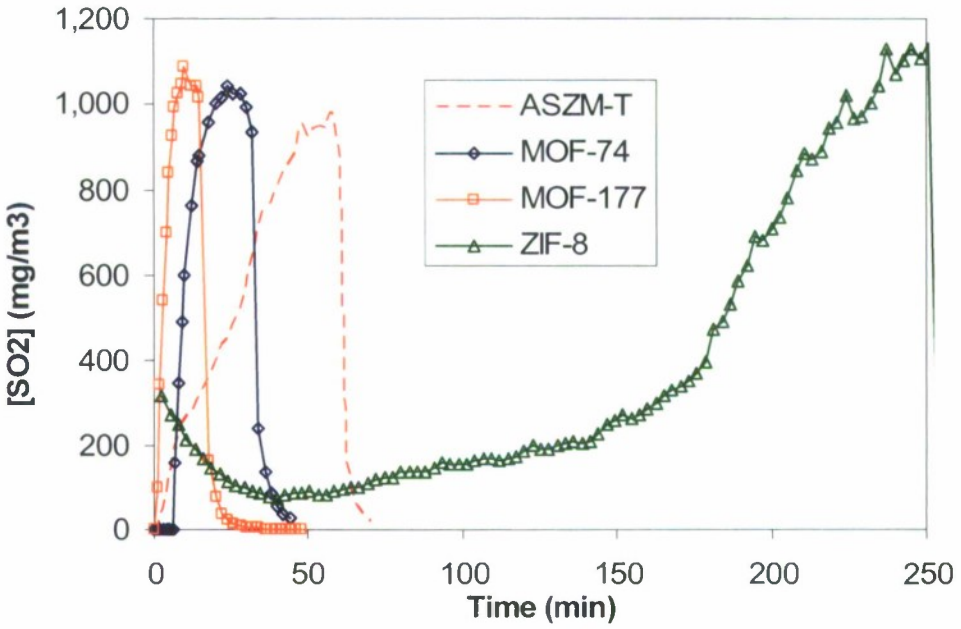

Figure 14. SO_2 Breakthrough Curves under Humid (RH = 80%) Conditions
[Challenge] = 1,000 mg/m^3

Under humid conditions, ASZM-TEDA and MOF-74 still provide SO_2 removal. Unlike dry RH conditions, however, these removal mechanisms are less reversible. The likely cause of this is a reaction between SO_2, oxygen and water to form sulfuric acid, the sulfate of which may be more strongly and/or irreversibly chemisorbed on the metals in each sorbent. Although MOF-177 does provide better SO_2 removal under humid conditions as compared to dry conditions, the capacity is significantly less than ASZM-TEDA. The performance of ZIF-8 is a surprise; although there is initial blow-by of the bed, possibly due to mass transfer limitations, ZIF-8 has a very high SO_2 capacity. This may be due to solution effects on the surface of ZIF-8. As more SO_2 goes into solution, the solution becomes more acidic and more favorable for additional SO_2 molecules. There may also be reaction within the supercages resulting in the formation of sulfuric acid, which is unable to desorb from the small pore apertures.

SO_2 breakthrough data were used to calculate the dynamic capacity using the same methodology used for ammonia. The results are summarized in Table 11.

4. SUMMARY

Two MOFs and one ZIF were evaluated for nitrogen, chloroethane, and water adsorption as well as ammonia, CK, and sulfur dioxide breakthrough behavior to determine appropriate design rules and synthesize subsequent samples for air purification applications. Table 12 summarizes the MOFs evaluated, their distinguishing characteristics, and properties associated with their structures.

Table 11. SO_2 Dynamic Capacity of Sorbents

Sample	Sorbent Mass* (mg)	Breakthrough Time to S.C. (min)	W_D to 500 mg/m^3	
			Mass Basis (g/g)	*Volume Basis** (g/cc)
MOF-74 (Dry)	15.3	11	0.014	0.006
MOF-74 (Wet)	19.2	9	0.009	0.004
MOF-177 (Dry)	15.3	1	0.001	<0.001
MOF-177 (Wet)	14.6	3	0.004	0.001
ZIF-8 (Dry)	18.6	1	0.001	<0.001
ZIF-8 (Wet)	15.3	138	0.226	0.129
ASZM-TEDA (Dry)	25.7	21	0.025	0.016
ASZM-TEDA (Wet)	56.1	27	0.105	0.065

*Dry basis – does not include mass of loaded water

Table 12. Comparison of Physical Properties of Sorbents Studied

Sample	Distinguishing Characteristic	BET Capacity	Pore Volume	Pore Width	Pore Aperture	H_2O Capacity @ 80% RH
		m^2/g	*g/cc*	*Å*	*Å*	*g/g*
MOF-5	Baseline IRMOF	3,290	1.34	11.0 & 15.1	7.8	0.10
IRMOF-3	IRMOF with amino-functionalized BBC linker	2,310	0.99	9.7 & 15.1	5.9 – 7.8	0.13
IRMOF-62	Interpenetrated IRMOF	2,550	1.09	TBD	TBD	0.03
MOF-199	Unsaturated copper sites	1,460	0.68	6.9, 11.1 & 13.2	4.1 & 6.9	0.46
MOF-74	Unsaturated zinc sites	990	0.48	10.8	10.8	0.32
MOF-177	Large linkers and very high surface area	4,065	1.73	11.8	9.6	0.14
ZIF-8	Sodalite zeolite structure	1,600	0.65	11.6	3.4	<0.01
ASZM-T	Activated carbon	820	0.46	Heterogeneous		0.28

Table 13 summarizes the ammonia, CK and SO_2 breakthrough capacities for the MOFs evaluated in this as well as previous efforts.

Table 13. Comparison of Removal Capacities of Sorbents Studied

Sample	Distinguishing Characteristic	NH_3 Capacity	CK Capacity	SO_2 Capacity
		g/g	*g/g*	*g/g*
MOF-5 (Dry)	Baseline IRMOF	0.02	< 0.01	< 0.01
MOF-5 (Wet)		0.19	< 0.01	< 0.01
IRMOF-3 (Dry)	IRMOF with amino-functionalized BBC linker	0.17	0.02	< 0.01
IRMOF-3 (Wet)		0.11	< 0.01	0.01
IRMOF-62 (Dry)	Interpenetrated IRMOF	0.10	0.02	< 0.01
IRMOF-62 (Wet)		0.08	< 0.01	< 0.01
MOF-199 (Dry)	Unsaturated copper sites	0.16	0.24	0.01
MOF-199 (Wet)		0.08	< 0.01	0.01
MOF-74 (Dry)	Unsaturated zinc sites	0.10	0.20	0.01
MOF-74 (Wet)		0.07	< 0.01	0.01
MOF-177 (Dry)	Large linkers and very high surface area	0.03	0.01	< 0.01
MOF-177 (Wet)		0.05	< 0.01	< 0.01
ZIF-8 (Dry)	Sodalite structure, small pores	< 0.01	< 0.01	< 0.01
ZIF-8 (Wet)		< 0.01	< 0.01	0.23
ASZM-T (Dry)	Activated carbon	0.02	0.14	0.02
ASZM-T (Wet)		0.03	0.17	0.11

Of the MOFs studied, unsaturated metal sites, generally leads to the highest adsorption capacities, but only at low humidity conditions. There are also other possible options utilizing the extremely large-pore IRMOFs as these show extensive ammonia removal capacities. Based on results from evaluating the MOFs and ZIF studied in this effort, several recommendations and possible approaches for synthesizing the next set of MOFs have been determined:

- Synthesize and evaluate additional MOFs with unsaturated metal sites, focusing on various metals for more extensive capacity and linkers that limit moisture adsorption.

- Investigate impregnation techniques on high porosity MOFs, focusing on the metal complexes found in ASZM-T as well as other formulations for additional ammonia removal capacity.

A preliminary approach has been identified consisting of two concurrent efforts. Figures 15 and 16 summarize the approach.

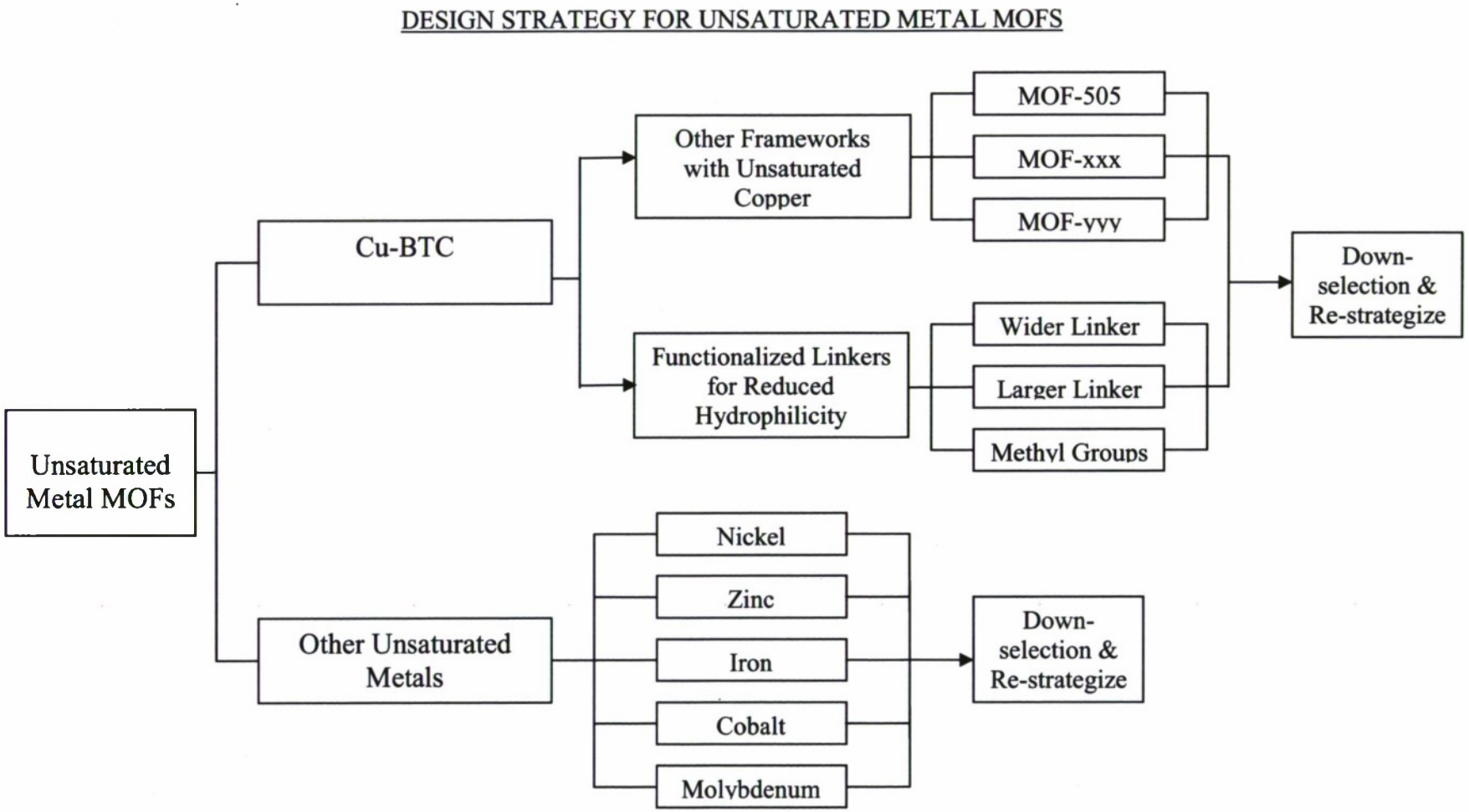

Figure 15. Design Strategy for Unsaturated Metal MOFs

DESIGN STRATEGY FOR ZINC OXIDE/ BDC ISORETICULAR MOFS

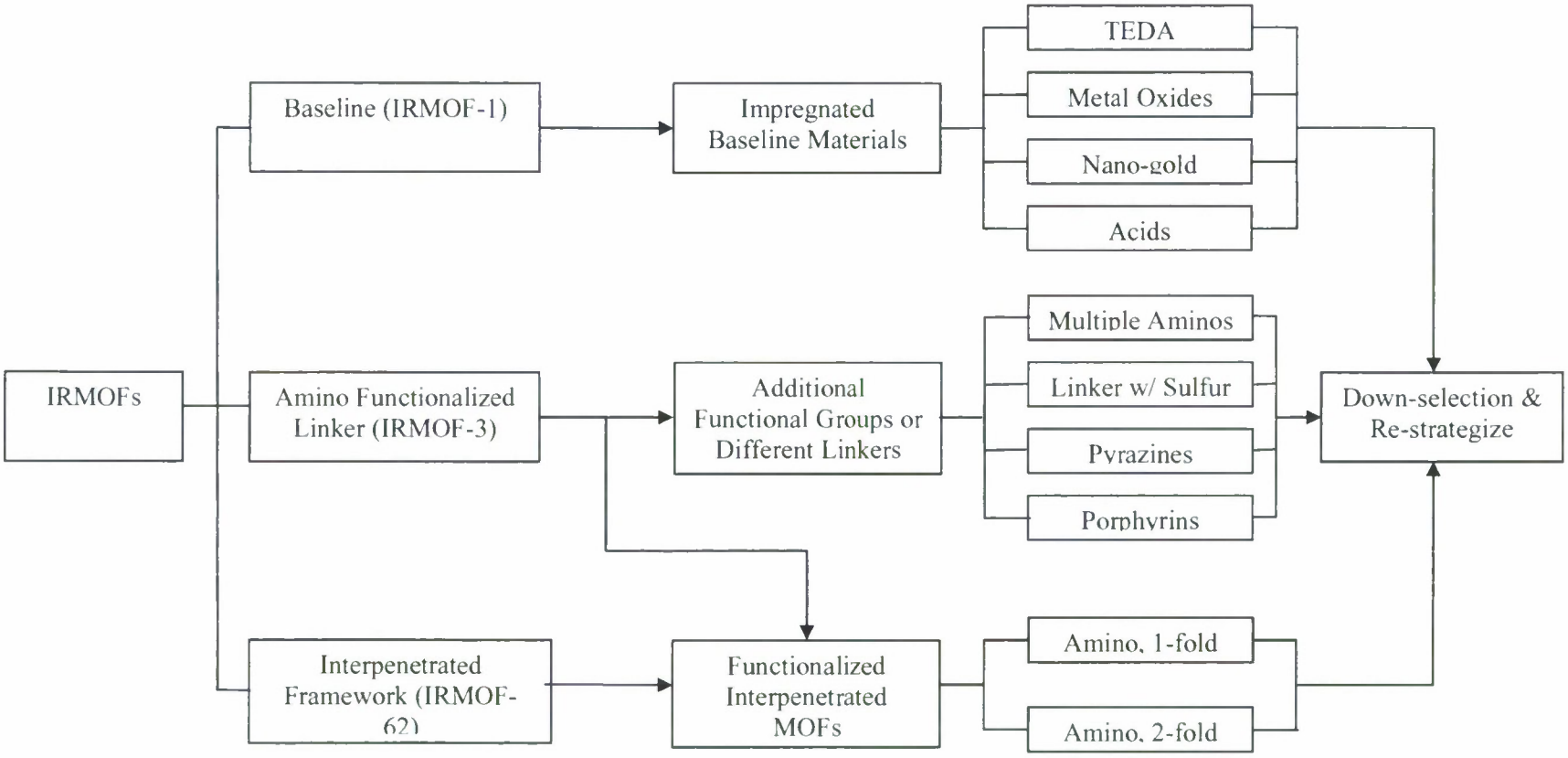

Figure 16. Design Strategy for IRMOFs

Blank

LITERATURE CITED

Peterson, G.W.; Mahle, J.J.; Balboa, A.; Sewell, T.L.; Karwacki, C.J.; Friday, D. *Evaluation of Metal-Organic Frameworks for the Removal of Toxic Industrial Chemicals*; ECBC-TR-621; U.S. Army Edgewood Chemical Biological Center: Aberdeen Proving Ground, MD, 2008; UNCLASSIFIED Report (AD A483 299).

Wong-Foy, A.G.; Matzger, A.J.; Yaghi, O.M. Exceptional H_2 Saturation Uptake in Microporous Metal-Organic Frameworks. *J. Am. Chem. Soc.* **2006**, *128*, 3494-3495.

Rosi, N.L.; Kim, J.; Eddaoudi, M.; Chen, B.; O'Keeffe, M.; Yaghi, O.M. Rod Packings and Metal-Organic Frameworks Constructed from Rod-Shaped Secondary Building Units. *J. Am. Chem. Soc.* **2005**, *127*, 1504-1518.

Rowsell, J.L.C.; Millward, A.R.; Park, K.S.; Yaghi, O.M. Hydrogen Sorption in Functionalized Metal-Organic Frameworks. *J. Am. Chem. Soc.* **2004**, *126*, 5666-5667.

Kim, J.; Chen, B.; Reineke, T.; Li, H.; Eddaoudi, M.; Moler, D.B.; O'Keeffe, M.; Yaghi, O.M. Assembly of Metal-Organic Frameworks from Large Organic and Inorganic Secondary Building Units: New Examples and Simplifying Principles for Complex Structures. *J. Am. Chem. Soc.* **2001**, *123*, 8239-8247.

Rowsell, J.L.C.; Yaghi, O.M. Effects of Functionalization, Catenation, and Variation of the Metal Oxide and Organic Linking Units on the Low-Pressure Hydrogen Adsorption Properties of Metal-Organic Frameworks. *J. Am. Chem. Soc.* **2006**, *128*, 1304-1315.

Park, K.S.; Ni, Z.; Cote; A.P.; Choi, J.Y.; Huang, R.; Uribe-Romo, F.J.U.; Chae, H.K.; O'Keeffe, M.; Yaghi, O.M. Exceptional Chemical and Thermal Stability of Zeolitic Imidazolate Frameworks. *PNAS* **2006**, *vol. 103,* no. 27, 10186-10191.

Liang, J.; Shimizu, G.K.H. Crystalline Zinc Diphosphonate Metal-Organic Framework with Three-Dimensional Microporosity. *Inorg. Chem.* **2007**, *46*, 10449-10451.

Li, Y.; Yang, R. Gas Adsorption and Storage in Metal-Organic Framework MOF-177. *Langmuir* **2007**, *23*, 12937-12944.

Li, H; Eddaoudi, M.; O'Keeffe, M.; Yaghi, O.M. Design and Synthesis of an Exceptionally Stable and Highly Porous Metal-Organic Framework. *Nature* **1999**, *402*, 276-279.

Chae, H.K.; Siberio-Perez, D.Y.; Kim, J.; Go, Y.; Eddaoudi, M.; Matzger, A.J.; O'Keeffe, M.; Yaghi, O.M. A Route to High Surface Area, Porosity and Inclusion of Large Molecules in Crystals. *Nature* **2004**, *427*, 523-527.

Park, K.S.; Ni, Z.; Cote, A.P.; Choi, J.Y.; Huang, R.; Uribe-Romo, F.J.; Chae, H.K.; O'Keeffe, M.; Yaghi, O.M. Exceptional Chemical and Thermal Stability of Zeolitic Imidazolate Frameworks. *PNAS* **2006**, *Vol. 103,* No. 27, 10186-10191.

Walton, K.S.; Snurr, R.Q. Applicability of the BET Method for Determining Surface Areas of Microporous Metal-Organic Frameworks. *JACS* **2007**.

Rouquerol, J.; Llewelly, P.; Rouquerol, F. Is the BET Equation Applicable to Microporous Adsorbents. *Studies in Surface Science and Catalysis* **2007,** *160*, 49-56.

Lowell, S.; Shields, J.; Thomas, M.; Thommes, M. *Characterization of Porous Solids and Powders: Surface Area, Pore Size and Density.* Kluwer Academic Publishers: Dordrech, The Netherlands, 2004.

APPENDIX A
PREVIOUS MOFS EVALUATED

MOF-5
($Zn_4O_{13}C_{24}H_{12}$)

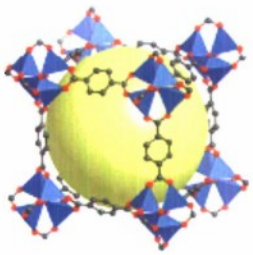

IRMOF-8
($Zn_4O_{13}C_{32}N_2H_{18}$)

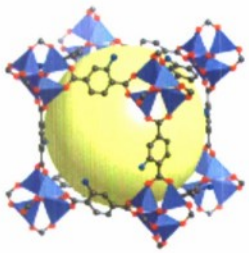

IRMOF-62
($Zn_4O_{13}C_{54}H_{30}$)

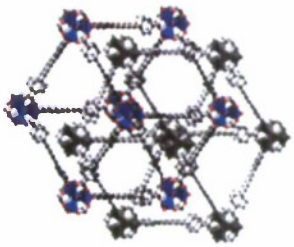

MOF-199
($CuO_4C_9H_6$)

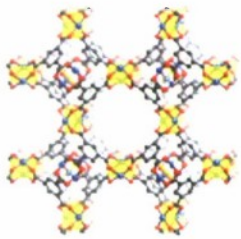

Blank

APPENDIX B
MOF SYNTHESIS TECHNIQUES

IRMOF-1 (MOF-5). "Triethylamine was mixed into a solution of zinc (II) nitrate and H_2BDC in *N,N'*-dimethylformamide (DMF)/chlorobenzene." (Li et al, 1999)

IRMOF-3. "2-Aminobenzene-1,4-dicarboxylic acid (0.75 g, 4.1 mmol, Aldrich) and zinc nitrate tetrahydrate (3.0 g, 11 mmol, EM Science) were dissolved in 100 mL of *N,N*-diethylformamide (BASF) with stirring in a 1 L wide mouth glass jar. The jar was tightly capped and placed in a 100 °C oven for 18 hr to yield cubic crystals. After decanting the hot mother liquor and rinsing with DMF, the product was immersed in chloroform (Fisher) for 3 days, during which the activation solvent was decanted and freshly replenished three times. The solvent was removed under vacuum at room temperature, yielding the porous material." (Rowsell and Yaghi, 2006)

IRMOF-62.

MOF-74. "Benzene-1,3,5-tricarboxylic acid (5.0 g, 24 mmol, Aldrich) and zinc nitrate tetrahydrate (10.0 g, 38 mmol, Aldrich) were dissolved in 500 mL of *N,N*-dimethylformamide (Fisher) in a 1 L wide mouth glass jar. After dissolution of the reagents, 25 mL of deionized water was added. The jar was tightly capped and placed in an 85 °C oven for 20 hr to yield trigonal block crystals. After decanting the hot mother liquor and rinsing with DMF, the product was immersed in methanol (Fisher) for 6 days, during which the activation solvent was decanted and freshly replenished three times. The solvent was removed under vacuum at 270 °C, yielding the porous material." (Rowsell and Yaghi, 2006)

MOF-177. "A solution of DEF containing 4,4',4"-benzene-1,3,5-triyl-tri-benzoic acid (H_3BTB; 5.00×10^{-3} g, 1.14×10^{-5} mol) and $Zn(NO_3)_2\ 6H_2O$ (0.020 g, 6.72×10^{-5} mol) was placed in a Pyrex tube of dimensions 10 mm (outer diameter), 8 mm (inner diameter), and 150 mm (length). The sealed tube was heated at a rate of 2.0 °C min^{-1} to 100 °C, held at 100 °C for 23 hr, and cooled at a rate of 0.2 °C min^{-1} to room temperature. Block-shaped crystals of MOF-177 were formed and isolated by washing with DEF (4 x 2 mL) and drying briefly in air (~1 min) (0.005 g, 32% based on H_3BTB)." (Chae et al, 2004)

MOF-199 (Cu-BTC, HKUST-1). "Benzene-1,3,5-tricarboxylic acid (5.0 g, 24 mmol, Aldrich) and copper (II) nitrate hemipentahydrate (10.0 g, 43 mmol, Aldrich) were stirred for 1 min in 250 mL of solvent consisting of equal parts *N,N*-dimethylformamide (Fisher), ethanol (Fisher), and deionized water in a 1 L wide mouth glass jar. The jar was tightly capped and placed in an 85 °C oven for 20 hr to yield small octahedral crystals. After decanting the hot mother liquor and rinsing with DMF, the product was immersed in dichloromethane (Fisher) for 3 days, during which the activation solvent was decanted and freshly replenished three times. The solvent was removed under vacuum at 170 °C, yielding the porous material." (Rowsell and Yaghi, 2006)

ZIF-8. "A solid mixture of zinc nitrate tetrahydrate $Zn(NO_3)_2 \cdot 4H_2O$ (0.210 g, 8.03×10^{-4} mol) and 2-methylimidazole (H-MeIM) (0.060 g, 7.31×10^{-4} mol) was dissolved in 18 mL of DMF in a 20-mL vial. The vial was capped and heated at a rate of 5 °C/min to 140 °C in a programmable oven and held at this temperature for 24 hr, then cooled at a rate of 0.4 °C/min to room temperature. After removal of the mother liquor from the mixture, chloroform (20 mL) was added to the vial. Colorless polyhedral crystals were collected from the upper layer, washed with DMF (10 mL x 3), and air dried for 10 min (yield: 0.032 g, 25% based on H-MeIM)." (Park et al, 2006)